Acta Pharmaceutica Sinica B 2022;12(4):1707−1722

Chinese Pharmaceutical Association
Institute of Materia Medica, Chinese Academy of Medical Sciences

Acta Pharmaceutica Sinica B

www.elsevier.com/locate/apsb
www.sciencedirect.com

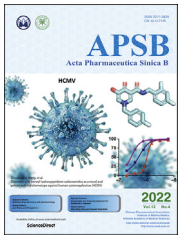

ORIGINAL ARTICLE

Celastrol enhances transcription factor EB (TFEB)-mediated autophagy and mitigates Tau pathology: Implications for Alzheimer's disease therapy

Chuanbin Yang[a,b,*,†], Chengfu Su[a,c,d,†], Ashok Iyaswamy[a,c,†], Senthil Kumar Krishnamoorthi[a,†], Zhou Zhu[a,c], Sichang Yang[a], Benjamin Chunkit Tong[a,c], Jia Liu[a,c], Sravan G. Sreenivasmurthy[a,c], Xinjie Guan[a], Yuxuan Kan[a], Aston Jiaxi Wu[a], Alexis Shiying Huang[a], Jieqiong Tan[e], Kingho Cheung[a,c], Juxian Song[a,f,*], Min Li[a,c,*]

[a]*Mr. & Mrs. Ko Chi-Ming Centre for Parkinson's Disease Research, School of Chinese Medicine, Hong Kong Baptist University, Hong Kong SAR, China*
[b]*Department of Geriatrics, Shenzhen People's Hospital (the Second Clinical Medical College, Jinan University; the First Affiliated Hospital, Southern University of Science and Technology), Shenzhen 518020, China*
[c]*Institute for Research and Continuing Education, Hong Kong Baptist University, Shenzhen 518057, China*
[d]*College of Pharmacy, Henan University of Chinese Medicine, Zhengzhou 450000, China*
[e]*Center for Medical Genetics and Hunan Key Laboratory of Animal Model for Human Diseases, School of Life Sciences, Central South University, Changsha 410078, China*
[f]*Medical College of Acupuncture-Moxibustion and Rehabilitation, Guangzhou University of Chinese Medicine, Guangzhou 510632, China*

Received 2 September 2021; received in revised form 11 December 2021; accepted 16 December 2021

KEY WORDS

TFEB;
Autophagy;
Lysosome biogenesis;

Abstract Alzheimer's disease (AD), characterized by the accumulation of protein aggregates including phosphorylated Tau aggregates, is the most common neurodegenerative disorder with limited therapeutic agents. Autophagy plays a critical role in the degradation of phosphorylated Tau aggregates, and transcription factor EB (TFEB) is a master regulator of autophagy and lysosomal biogenesis. Thus, small-molecule autophagy enhancers targeting TFEB hold promise for AD therapy. Here, we found that

*Corresponding authors. Tel.: +86 852 3411 2919; fax: +86 852 3411 2461.
E-mail addresses: limin@hkbu.edu.hk (Min Li), juxian.song@gmail.com (Juxian Song), nkyangchb@gmail.com, h1094103@connect.hku.hk (Chuanbin Yang).
[†]These authors made equal contributions to this work.
Peer review under responsibility of Chinese Pharmaceutical Association and Institute of Materia Medica, Chinese Academy of Medical Sciences.

https://doi.org/10.1016/j.apsb.2022.01.017

Alzheimer's disease (AD);
Tau;
Celastrol;
mTOR;
Therapeutic target

celastrol, an active ingredient isolated from the root extracts of *Tripterygium wilfordii* (Lei Gong Teng in Chinese) enhanced TFEB-mediated autophagy and lysosomal biogenesis *in vitro* and in mouse brains. Importantly, celastrol reduced phosphorylated Tau aggregates and attenuated memory dysfunction and cognitive deficits in P301S Tau and 3xTg mice, two commonly used AD animal models. Mechanistical studies suggest that TFEB-mediated autophagy-lysosomal pathway is responsible for phosphorylated Tau degradation in response to celastrol. Overall, our findings indicate that Celastrol is a novel TFEB activator that promotes the degradation of phosphorylated Tau aggregates and improves memory in AD animal models. Therefore, Celastrol shows potential as a novel agent for the treatment and/or prevention of AD and other tauopathies.

1. Introduction

Alzheimer's disease (AD) is the most common neurodegenerative disorder in the world. According to the *2020 Alzheimer's Disease Facts and Figures* report, about 10% of people above the age of 65 are living with AD in the United States[1]. Unfortunately, currently available medications for AD are very limited; most drugs only offer moderate symptomatic relief and have side effects. Therefore, novel effective drugs are urgently needed. The key histopathological features of AD include senile plaques formed by the accumulation of amyloid β-peptide (Aβ), and neurofibrillary tangles comprising phosphorylated, misfolded Tau aggregates[2–4]. In the past decades, most drugs developed to treat AD by targeting Aβ have not demonstrated promising clinical efficacy. Biogen's monoclonal antibody aducanumab targeting Aβ has recently been approved by U.S. Food and Drug Administration (FDA); however, whether aducanumab improves cognitive decline is controversial[5]. New approaches that target phosphorylated Tau have received increasing attention because the Tau pathology is tightly linked to memory deficits in AD[6,7]. Among all the strategies that target Tau protein aggregates, activating macroautophagy (hereafter referred to as autophagy) to promote Tau aggregates degradation is considered as the most effective approach.

Autophagy is a conserved catabolic pathway for the degradation of long-lived proteins, protein aggregates, and organelles (*e.g.*, mitochondrial) by lysosomes[8–10]. Autophagy dysfunction is involved in the pathology of a variety of diseases including neurodegenerative diseases[11–15]. The multiple stages of autophagy impairment involve in autophagosome maturation, autophagosome formation, and autophagosome–lysosome fusion has been implicated in the pathogenesis of AD[16]. Several AD-associated genes such as presenilin 1, presenilin 2, and phosphatidylinositol binding clathrin assembly protein have been shown to affect autophagy and/or lysosome functions[10,17,18]. We and others recently found that nuclear receptor-binding factor 2 (*NRBF2*), a main component of the class III phosphatidylinositol 3-kinase (PtdIns3K) complex, is reduced in the hippocampus of 5XFAD transgenic mice and AD patients[19,20]. In mouse models, NRBF2 deficiency affects memory and exaggerates AD-like pathology[19–21]. Mechanistically, NRBF2 modulates autophagosome formation and autophagosome–lysosome fusion and interacts with amyloid beta precursor protein (APP) to regulate APP-CTFβ degradation and subsequent Aβ homeostasis in an autophagy-dependent manner[19,22]. The expressions of other autophagy-related proteins such as Beclin 1[13,23] are also reduced in AD patients and transgenic mice. Deletion of Beclin 1 increases both the intracellular Aβ and extracellular Aβ and accelerates AD progress[13]. Additionally, deficiency in essential autophagy-related genes such as *ATG7* affects both Aβ production and secretion in AD mouse models[24,25]. Conversely, genetic or pharmacological induction of the autophagy–lysosome pathway ameliorates the pathological features associated with AD[13,26]. These results highlight a pivotal role of autophagy in AD pathogenesis.

Previously, TFEB has been known as the main regulator of autophagy lysosomal pathway[27–29]. It has been demonstrated overexpression of TFEB enhances autophagy, thereby promoting Tau degradation, restoring normal neural function, and rescuing behavioral deficits in multiple AD animal models[3,30,31]. Thus, targeting TFEB-mediated autophagy to enhance the clearing of Tau aggregates represents a promising strategy for AD treatment. However, high potency TFEB small molecule activators are rarely reported. Moreover, poor blood–brain barrier (BBB) permeability of current known TFEB activators hinders their application for treating neurodegenerative diseases including AD.

Celastrol is a leptin sensitizer, initially isolated from the roots of *Tripterygium wilfordii* (Lei Gong Teng, common name, thunder god vine). *T. wilfordii* is widely used in clinical for treating many diseases including rheumatoid arthritis and systemic lupus erythematosus in China[32]. As a main active compound of *T. wilfordii*, celastrol has multiple therapeutic activities such as anti-obesity and anti-inflammatory effects[32–35]. However, the role of celastrol in activating TFEB-mediated autophagy, lysosomal biogenesis, and promoting phosphorylated Tau degradation has not been reported. In searching for novel TFEB activators, we found that celastrol promotes TFEB translocation from the cytoplasm into the nucleus *in vitro* and *in vivo*, specifically in animal brains. Consequently, autophagy and lysosomal biogenesis were enhanced. Given that TFEB activation could promote Tau aggregate degradation and alleviate AD-like pathology in animal models, in our study, we tested the effectiveness of celastrol on attenuating Tau pathology in P301S and 3xTg AD mice and then investigated the underlying mechanism. Our results show that celastrol is a novel TFEB activator that promotes the degradation of phosphorylated Tau aggregates and improves memory deficiency in AD animal models. The findings from this study provide key evidence for future clinical development of celastrol as a novel agent for the treatment and/or prevention of AD and other tauopathies.

2. Materials and methods

2.1. Chemical and reagents

Tau antibodies used in this study PHF1, CP13, and MC1 were generously gifted by Prof. Peter Davies, Albert Einstein College, NY, USA. Torin 1 (2273-5) was purchased from BioVision Inc. Bafilomycin A1 (sc-201550) and anti-β-actin/ACTB (sc-47778) were obtained from Santa Cruz Biotechnology. The following primary antibodies were used: Flag M2 (Sigma−Aldrich, F1804); Phospho-ribosomal protein S6 kinase B1 (P70S6K/RPS6KB1, Thr389; Cell Signaling Technology, 9234); P70S6K/RPS6KB1 (Cell Signaling Technology, 9202); H3F3A/histone H3 (D1H2; Cell Signaling Technology, 4499); microtubule-associated protein 1 light chain 3B (LC3B; Novus Biologicals, NB100-2220); TFEB (Bethyl Laboratories, A303-673A); anti-phospho-TFEB (Ser142; Millipore, ABE1971); anti-phospho-TFEB (Ser211; Cell Signaling Technology, 37681S); GAPDH antibody (GeneTex, GTX100118). The following items were used: Alexa Fluor® 488 goat anti-mouse IgG (Life Technologies, A-11001); goat anti-rabbit IgG (Life Technologies, A-11034); vector ABC staining kit (PK-6100 Elite); chloroquine (C6628, Sigma−Aldrich); DAB Peroxidase Substrate Kit (VECTOR, SK-4100); protease inhibitor mixture (04693124001, Roche Applied Science); phosphatase inhibitor (B15001, Biotool); ECL kit (32106, Pierce); BAPTA acetoxymethyl ester (Sigma−Aldrich, A1076); okadaic acid (Sigma−Aldrich, 459620); Lysotracker® Red DND-99 (L-7528), FK-506 (sc-24649A), cyclosporin A (sc-3503) (Life Technologies); goat anti-rabbit (111-035-003) secondary antibodies, HRP-conjugated goat anti-mouse (115-035-003) (Jackson Immuno Research); RIPA lysis buffer (9803, Life Technologies); Trizol (15596026, Thermo Fisher Scientific). Celastrol was obtained from Aktin Chemical (Chengdu, China) with a purity of more than 98%.

2.2. Cell culture

HeLa, N2a, and HEK293 cells were maintained in Dulbecco's modified Eagle's medium (DMEM). HeLa cells stably expressing 3XFlag-TFEB (CF-7)[27,36,37] were cultured in DMEM containing 10% FBS and 200 μg/mL G418. RNAi-mediated knockdown experiments were conducted using Lipofectamine RNAiMAX (13778030) from Invitrogen. For overexpression experiments, cell transfection was used Lipofectamine 3000 (L3000015, Invitrogen) 3XFlag-TFEB plasmid was a kind gift from Professor Andrea Ballabio (TIGEM)[27,36,37]. 3XFlag-TFEB S142D and S211D plasmids were generated by using Q5® Site-Directed Mutagenesis Kit (NEB, E0554S) according to the manufacturer's instructions followed by verification using sequencing.

2.3. Animals and drug treatments

All animal experiments were approved by the Committee of Human & Animal Subjects in Teaching and Research (HASC), Hong Kong Baptist University (Hong Kong, China). We followed the approved protocols in all animal experiments. Animals were maintained at 23 ± 2 °C, 60 ± 15% relative humidity with 12-h light/dark cycles, and water and food were provided *ad libitum*. Homozygous human P301S Tau transgenic mice were kind gifts from Dr. Michael Goedert[38]. 1.5-Month-old mice (both male and female n = 7−8) were treated daily with celastrol at the concentrations of 1 and 2 mg/kg/day or vehicle for 2.5 months. Homozygous 3xTg mice bought from Jackson Laboratory (CA, USA) were used in this study. Since previous findings suggested that male 3xTg mice may not exhibit AD-like pathology[39], only female mice were used in our study. In 3xTg mice, celastrol was given daily from 6 months of age till the mice reached 15 months of age with concentrations of 1 and 2 mg/kg/day (n = 8 per group). For long-term treatment of celastrol to avoid oral damage, we mixed celastrol in regular feed as per our previous protocol; fresh feed containing celastrol was prepared twice weekly[40,41]. Briefly, the average daily amount of drug consumption was calculated based on the amount of food consumed every day. The assessment of animals' body weight and calculation of feed consumption were performed every 2 weeks. Celastrol was suspended in distilled water and mixed with the measured weight of regular feed powder. The mixture was kept at 55 °C to evaporate excessive water. A fresh feed with the required amount of celastrol was prepared twice weekly.

2.4. Open field test

Open field test was conducted as described previously[40−42]. Briefly, mice were placed in a plexiglass box (25 cm × 25 cm) and allowed to explore the environment. The behavior of each mouse was recorded for 5 min to analyze the exploratory and locomotor function. Time spend in center and margin were recorded and data analyzed as described in our previous reports[40,41].

2.5. Contextual fear conditioning (CFC) test

CFC test was performed according to previously described protocols[43]. Briefly, in two sound-proof chambers, all the experiments were conducted with continuous 40 units of white noise and 40 lux white light. In training experiments, mice were allowed to explore the platform for 2.5 min and then received three repeated foot shock cycles (30 s) at 30 s intervals, each starting with a cue tone (28 s, 1500 Hz) and ending with a foot shock (30.0 mA, 2 s). On the second day, the mice were allowed to explore the platform for 3 min followed by a cue tone (30 s, 1500 Hz) stimulation without foot shock, and the freezing time was recorded. Contextual fear memory formation and the subsequent remote memory stabilization were evaluated by scoring freezing index (the absence of all but respiratory movement).

2.6. The Morris water maze

The Morris water maze test was performed according to a previous protocol[44]. The data were analyzed as described in our previous reports[40,41]. Briefly, the hidden-platform training (4 trials/day) was performed for 6 consecutive days. The visible platform training was done with a flag attached to the platform, and the platform position was changed for each trial during the training session. The hidden-platform training included 4 trials per day, and every trial included four 60-s trials with a 30-min interval. In the hidden platform sessions, the platform location remained constant and the entry point for placing the mice in the tank was changed randomly between the training days. On the 7th day, a probe trial was conducted and allowed the mice to search for the platform for 60 s. The percentage of time spent in each quadrant and distance to reach the target quadrant of the pool during the probe trial was recorded and analyzed using an Ethovision video

tracking system (Version 3.0, Noldus Information Technology, Leesburg, VA, USA).

2.7. Western blotting analysis

Cells were lysed in RIPA to separate cytosol and nucleus extracts prepared according to our previous protocol[45−47]. The extracted protein was analyzed using Western blot, the protein was run in SDS-PAGE separating them at different kDa. The protein from the gel was transferred to the membrane and was probed for different proteins using a primary antibody and secondary antibody. The protein expression was detected using an ECL reagent and developed in the X-ray film.

2.8. Tau extraction

Sarcosyl-soluble and -insoluble Tau fractionation was performed based on our previous studies[40,41]. Briefly, brain samples were homogenized using lysis buffer containing protease and phosphatase inhibitor tablets. Soluble and insoluble pellets were obtained after centrifugation. The pellet fraction was extracted in a high salt lysis buffer. After 30 min centrifugation, 1% sarcosyl was mixed with the supernatant and incubated at RT for 2 h and centrifuged again for 30 min to separate sarcosyl-insoluble Tau in the pellet. The pellet was then resuspended in 20 μL of Tris-EDTA buffer. Total lysis buffer fraction, S1 fraction, and sarcosyl insoluble fractions were used for immunoblotting detection of human total Tau and phospho-Tau variants.

2.9. Immunohistochemistry

The extracted brain was cut into equal halves and one half was fixed in 4% paraformaldehyde and dehydrated in 30% sucrose. Then the brain was cut into slices in cryotome, and the brain slices were used for free-floating immunohistochemistry. The brain slices were permeated in 0.4% PBST for 15 min and further washed in 1 × PBS twice. Then brain slices were incubated in 5% BSA for 30 min at room temperature. Next, the target primary antibody was added to the free-floating brain slices and incubated overnight at 4 °C. The next morning the primary antibody was collected, and the brain slices were washed twice with PBS. Then secondary antibody with a fluorescent tag was incubated with brain slices for 2 h at room temperature. Next, the brain slices were washed with PBS and incubated with DAPI for 5 min and immediately washed twice with PBS. Then the brain slices were mounted in the slides, air-dried, and covered with a coverslip. The target brain fluorescence was imaged in confocal and analyzed for the intensity using Image J.

2.10. Flow cytometry assay

Lysotracker red staining was conducted as described previously[48] and by following the manufacturer's instructions. The lysotracker fluorescence intensity was detected using flow cytometry (BD Accuri C6 Plus). To analyze the data FlowJo software was used.

Venus-based Tau-BiFC system was constructed as described previously[49]. In this system, wild-type full-length human Tau or P301S mutation human Tau were fused to a non-fluorescent N-terminal fragment of Venus (VN173, 1−172 a.a.) and non-fluorescent C-terminal fragment of Venus (VC155, 155−238 a.a.). After transfection into cells, the fluorescence intensity could be used as an indicator for Tau aggregate formation. The BiFC fluorescence intensity was detected using flow cytometry (BD Accuri C6 Plus).

2.11. Quantitative real-time PCR

Total RNA was extracted from cells with the Trizol reagent. Reverse transcription was carried out following the protocol of the High-Capacity cDNA Reverse Transcription Kit (4368814, Life Technologies). The related gene primers of autophagy were followed with our previous research[37]. The primers were synthesized by Life Technologies, the primer sequences are listed in Supporting Information Table S1. Real-time PCR was performed using the Fast SYBR Green Master Mix (Life Technologies, 4385612) with the ViiA™ 7 Real-Time PCR System (Life Technologies, Carlsbad, CA, USA). Fold changes were calculated with the ΔΔCT method, and the results were normalized against an internal control (GAPDH).

2.12. Immunocytochemistry

The treated cells and control cells were fixed in 4% paraformaldehyde for 15 min and then permeabilized in 0.4% PBST for 15 min and further washed in 1 × PBS twice. Then cells were incubated in 5% BSA for 30 min at room temperature. Next, the target primary antibody was added to the cells and incubated overnight at 4 °C. After staining with anti-Flag primary antibody, the Alexa Fluor® 488 (green) secondary antibodies were added and incubated for 2 h. Next, the cells were labeled with DAPI and mounted in slides. The cells were visualized using an API Delta Vision Personal Imaging System and quantified using Image J.

2.13. Statistical analysis

All data are presented as mean ± standard error of mean (SEM) using GraphPad Prism 8.0. For *in vitro* experiments the drug treatment and untreated cells were compared using Student's *t*-test. For animal experiments, between groups comparison, and between animals were compared using one-way ANOVA. For behavior studies, we also used two-way ANOVA for some parameters to compare between groups at different time points and between animals. We used the Bonferroni test and Tukey's multiple comparison test for comparing the groups in the study.

3. Results

3.1. Celastrol activates TFEB to promote autophagy

By using HeLa cells stably expressing 3XFlag-TFEB (CF-7 cells) as a cell model, we evaluated several natural compounds for their ability to promote the accumulation of TFEB in the nucleus, and we found that celastrol (Cel, Fig. 1A) promoted TFEB translocation from the cytosol into the nucleus in a dose- (Fig. 1B and C) and time-dependent manner (Supporting Information Fig. S1A). Notably, celastrol is highly potent TFEB activation being achieved even at low micromolar concentrations (Fig. 1B and C). Since TFEB is a key regulator of autophagy and lysosomal biogenesis[27,29,50], we first identified the effect of celastrol on inducing autophagy by detecting the levels of a well-defined autophagy marker LC3B-II. As shown in Fig. 1D, celastrol increased LC3B-II levels. Celastrol also increased LC3B-II levels in the presence of lysosome inhibitor chloroquine (CQ, Fig. 1E), indicating that celastrol promotes autophagy flux rather than

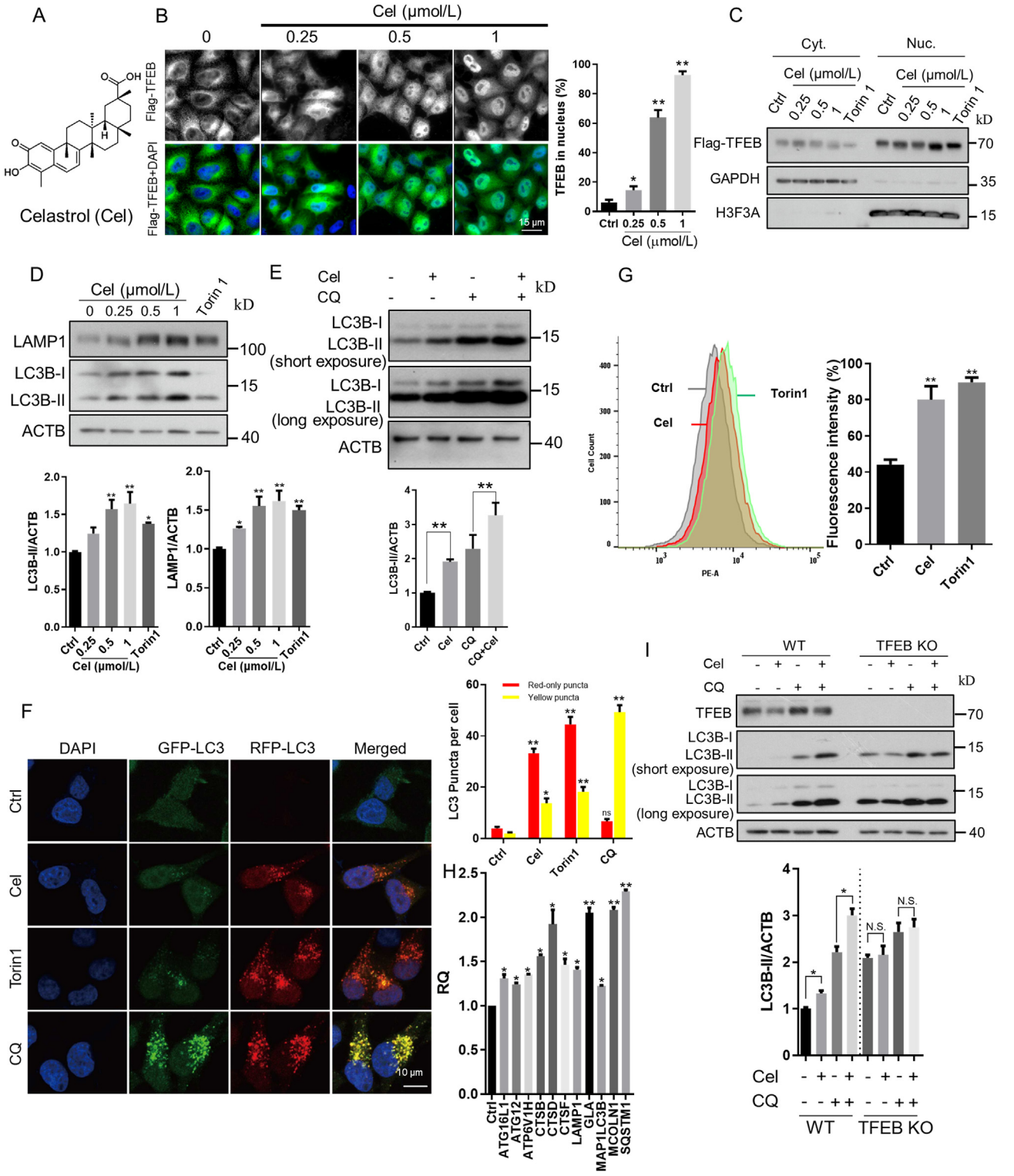

Figure 1 Celastrol promotes TFEB-mediated autophagy and lysosome biogenesis. (A) Chemical structure of celastrol (Cel). (B, C) Celastrol promotes TFEB translocation from the cytoplasm into the nucleus in HeLa cells stably expressing 3xFlag-TFEB as reflected by immunostaining and Western blot analysis (at least 250 cells were counted for each group, scale bar = 15 μm). (D) Celastrol increased the levels of LC3B-II and LAMP1. (E) Celastrol further increased LC3B-II levels in the presence of lysosome inhibitor CQ (chloroquine). (F) tf-LC3 staining further confirmed that celastrol promoted autophagy flux (scale bar = 10 μm). (G) Celastrol increased lysosomal numbers as reflected by Lysotracker Red DND-99 staining using flow cytometry assay. The TFEB activator Torin 1 was used as a positive control. (H) Celastrol increased the expression of multiple autophagy−lysosome-related genes as reflected by qPCR assay. (I) Knockout of the expression of TFEB attenuated celastrol-induced autophagy flux. All the values are average ± SEM from at least three independent experiments. $*P < 0.05$, $**P < 0.01$ *vs.* the control group or as indicated analyzed by one-way ANOVA.

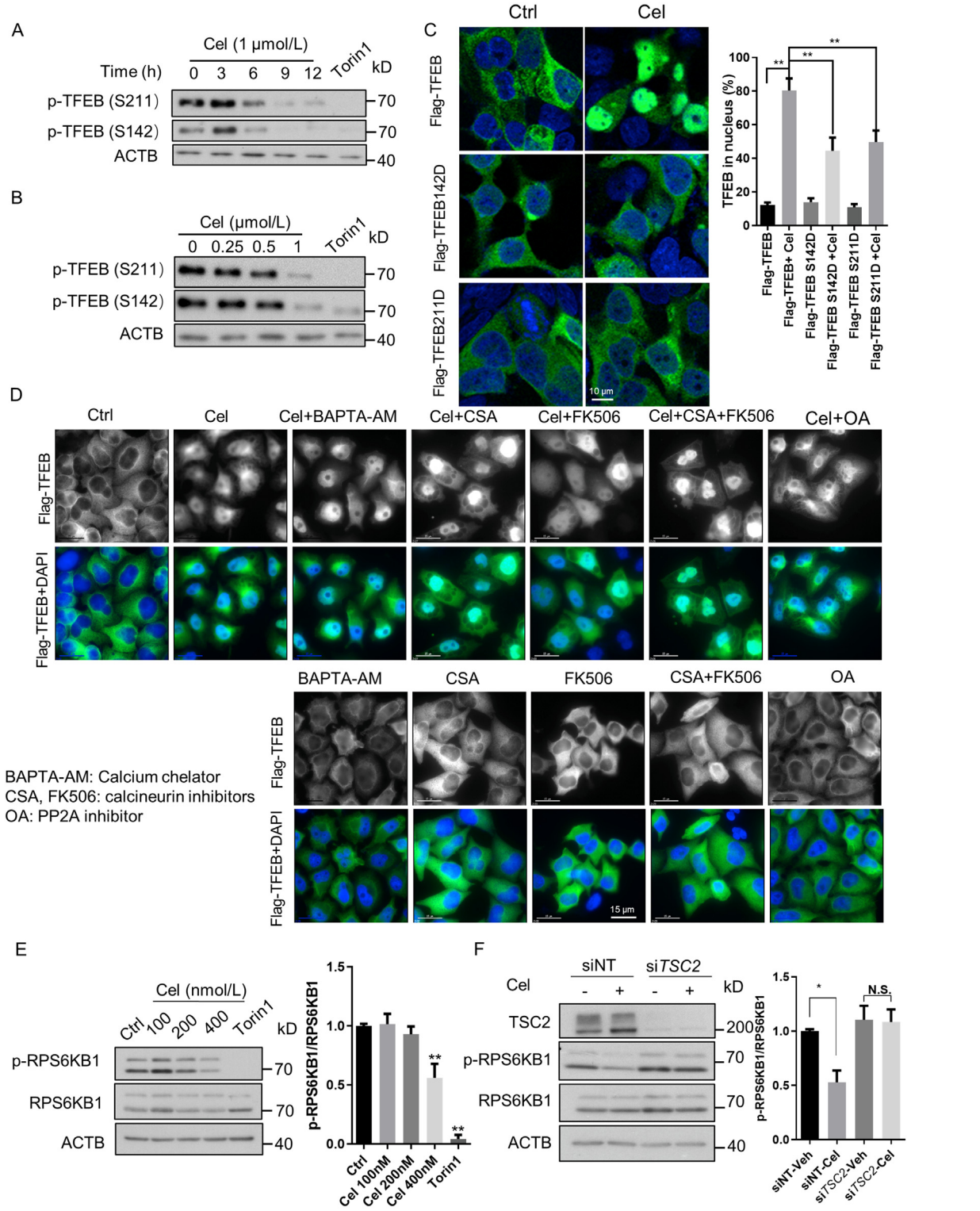

Figure 2 Celastrol promotes the nucleus accumulation of TFEB *via* mTORC1 inhibition. (A, B) Celastrol inhibited the phosphorylation of TFEB (Ser142 and Ser211) in a time- and dose-dependent manner in CF7 cells. (C) Transfection of HEK293 cells with two phosphomimetic TFEB mutants [TFEB(S142D), TFEB(S211D)] inhibited nuclear translocation of TFEB after celastrol treatment (scale bar = 10 μm). (D) After pretreatment of CF7 cells with calcium chelator BAPTA-AM (20 μmol/L), calcineurin inhibitors FK506 (10 μmol/L) and CSA (cyclosporin A, 20 μmol/L), or PP2A inhibitor OA (okadaic acid, 400 nmol/L) for 30 min and then followed with celastrol for another 9 h, the results show that these inhibitors did not attenuate celastrol-induced nuclear accumulation of TFEB. (E) Celastrol inhibited the phosphorylation of RPS6KB1 in HEK293 cells. (F) Knockdown of *TSC2* attenuated celastrol-induced dephosphorylation of mTORC1 substrate RPS6KB1. All the values are average ± SEM from at least three independent experiments. $^{*}P < 0.05$, $^{**}P < 0.01$ *vs.* the control group or as indicated analyzed by one-way ANOVA.

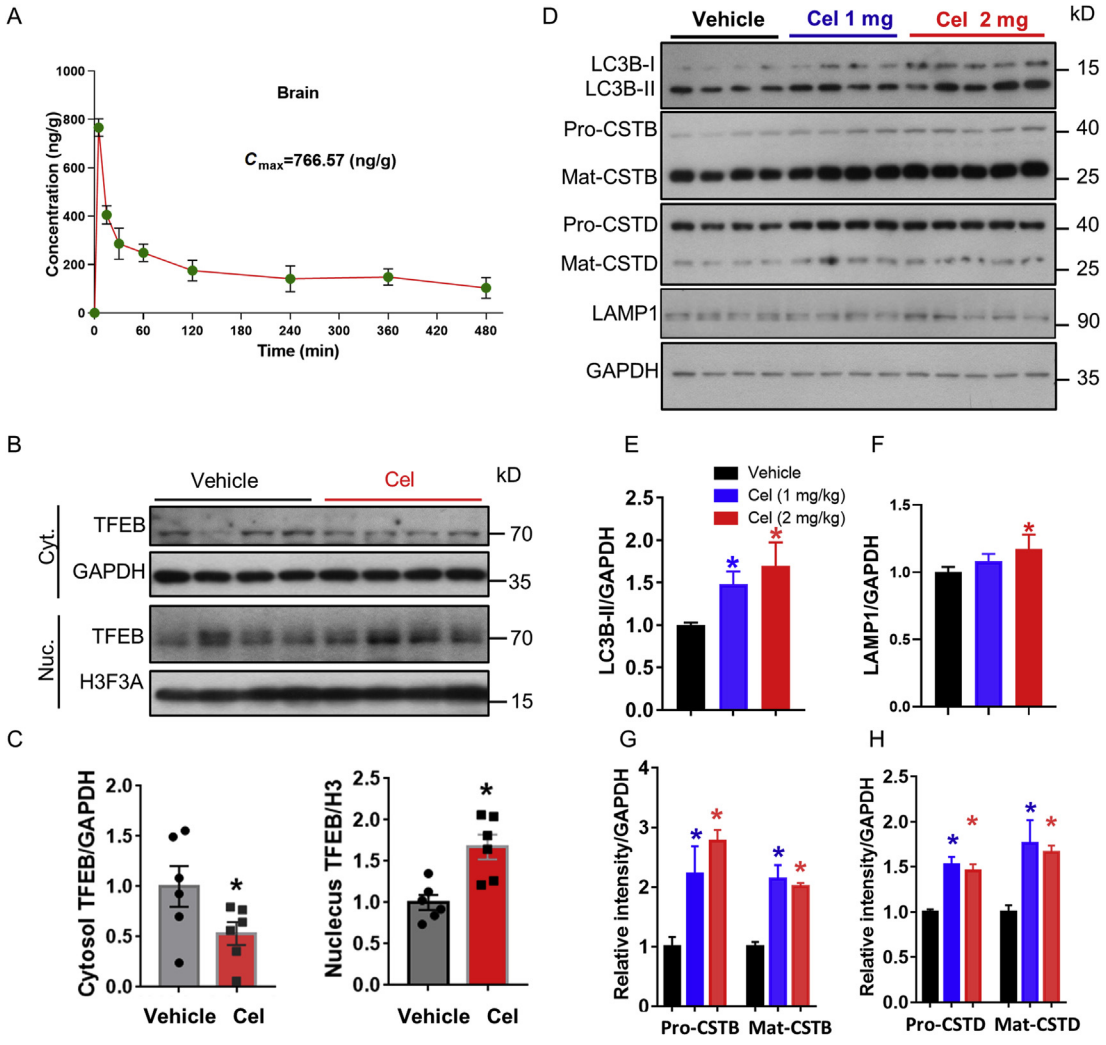

Figure 3 Celastrol is a blood−brain barrier permeable and enhances autophagy and lysosomal biogenesis in mouse brains. (A) Celastrol is brain permeable. Celastrol concentration in the brain was determined by LC−MS methods after giving mice 2 mg/kg celastrol by gavage. C_{max} = 766.67 ng/g (n = 5). C57 mice received 1 and 2 mg/kg/day celastrol for 7 consecutive days by gavage. (B, C) Celastrol promoted TFEB translocation from the cytoplasm into the nucleus in animal brains. (D−H) Celastrol increased autophagy and lysosome biogenesis. The expression of LC3B-II, LAMP1, cathepsin B, and cathepsin D in the frontal cortex was examined by Western blotting after treatment with celastrol. All the values are average ± SEM (n = 4−6). *P < 0.05 *vs.* Vehicle group analyzed by one-way ANOVA.

inhibiting lysosome functions. Microscope images showed red-only puncta of tfLC3 (Tandem RFP-LC3-GFP) constructs[51] were increased, further confirming that celastrol promotes autophagy flux (Fig. 1F). Importantly, celastrol increased lysosomal contents as proved by Lysotracker Red staining (Fig. 1G). We further showed that celastrol increased the lysosomal-associated membrane protein 1 (LAMP1) levels (Fig. 1D) and induced the expression of multiple genes related to autophagy and the lysosome pathway (Fig. 1H). Importantly, the knockout of *TFEB* attenuated celastrol-induced autophagy flux (Fig. 1I). Taken together, these results indicate that celastrol enhances TFEB-mediated autophagy and lysosomal biogenesis.

3.2. Celastrol activates TFEB via inhibiting mammalian target of rapamycin complex 1 (mTORC1)

To investigate the possible mechanisms by which celastrol promotes the nuclear accumulation of TFEB, we first determined the role of celastrol in TFEB phosphorylation status, which is critical for TFEB subcellular localization. As shown in Fig. 2A and B, celastrol induced the dephosphorylation of TFEB (S142 and S211) in a time- and dose-dependent manner. Furthermore, after transfection of cells with two phosphomimic TFEB mutants [TFEB(S142D), TFEB(S211D)] in HEK293 cells, we found that the nuclear translocation of TFEB after celastrol treatment was compromised (Fig. 2C), suggesting that the dephosphorylation of TFEB at S142 and S211 is important for the nuclear translocation of TFEB. Certain phosphatases namely calcium-dependent PPP3/calcineurin, an endogenous serine/threonine phosphatase, can dephosphorylate TFEB[45,52,53] and translocate from the cytosol into the nucleus. Therefore, we wanted to check whether calcineurin is required for celastrol-induced nuclear accumulation of TFEB. In Fig. 2D, cells were pretreated with PPP3/calcineurin inhibitor CsA (cyclosporin A) and FK506[54] or calcium chelator BAPTA-AM (BAPTA acetoxymethyl ester) did not obviously inhibit the nuclear translocation of TFEB after celastrol treatment

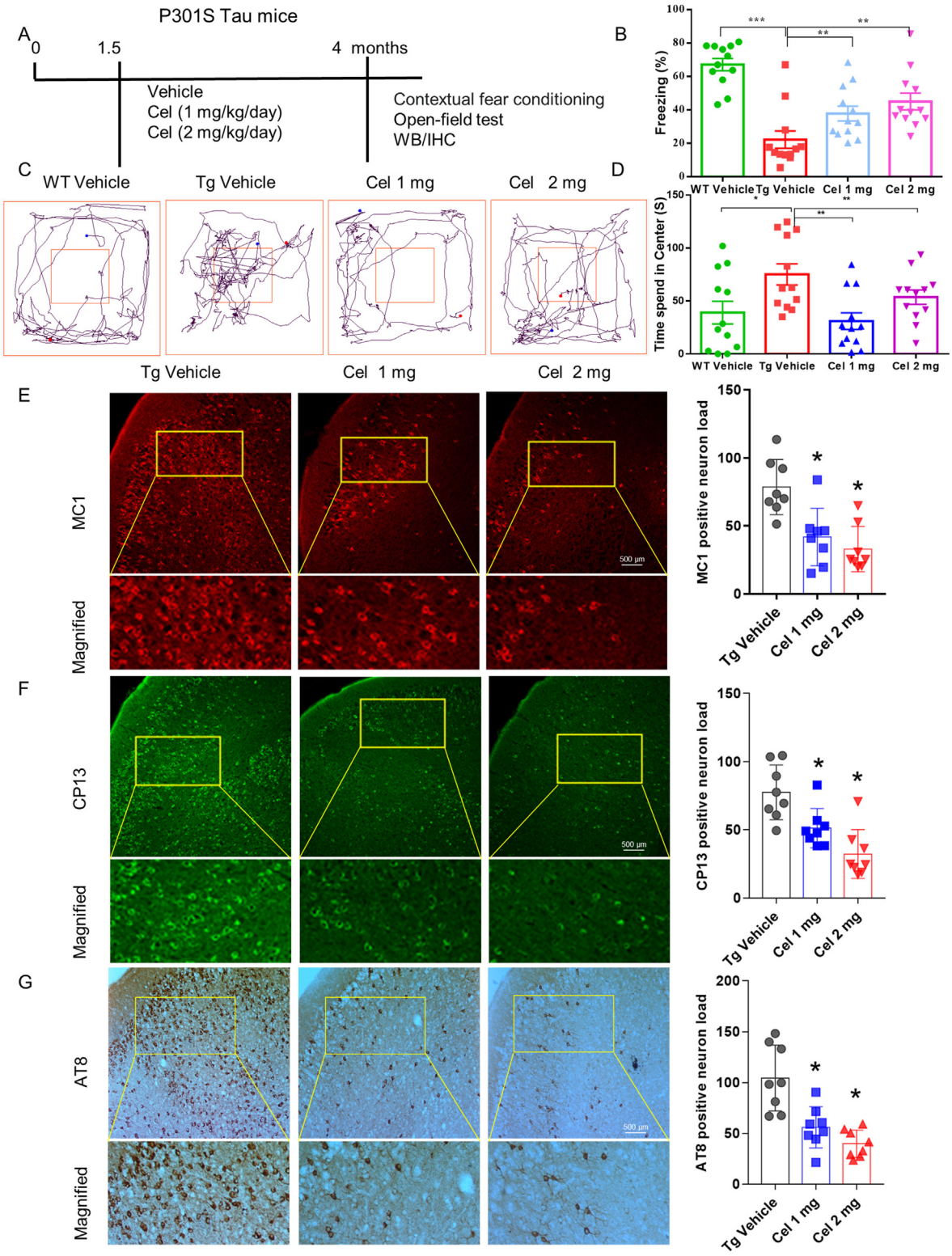

Figure 4 Celastrol ameliorates memory impairment and reduces phosphorylated Tau aggregates in P301S Tau mice. (A) Schematic models show experimental design for P301S Tau mice. At the end of celastrol treatment, (B) contextual fear conditioning test results show that celastrol improved memory impairments. (C, D) Open field test results show that celastrol improved exploratory and locomotor behavior. (E) Immunofluorescence analysis and quantification data show that celastrol reduced MC1 levels. (F) Immunofluorescence analysis and quantification data show that celastrol reduced CP13 levels. (G) Immunohistochemistry analysis and quantification data show that celastrol reduced AT8 levels (scale bar = 500 μm). All the values are average ± SEM (n = 7−8). *P < 0.05, **P < 0.01 *vs.* Vehicle group analyzed by one-way ANOVA.

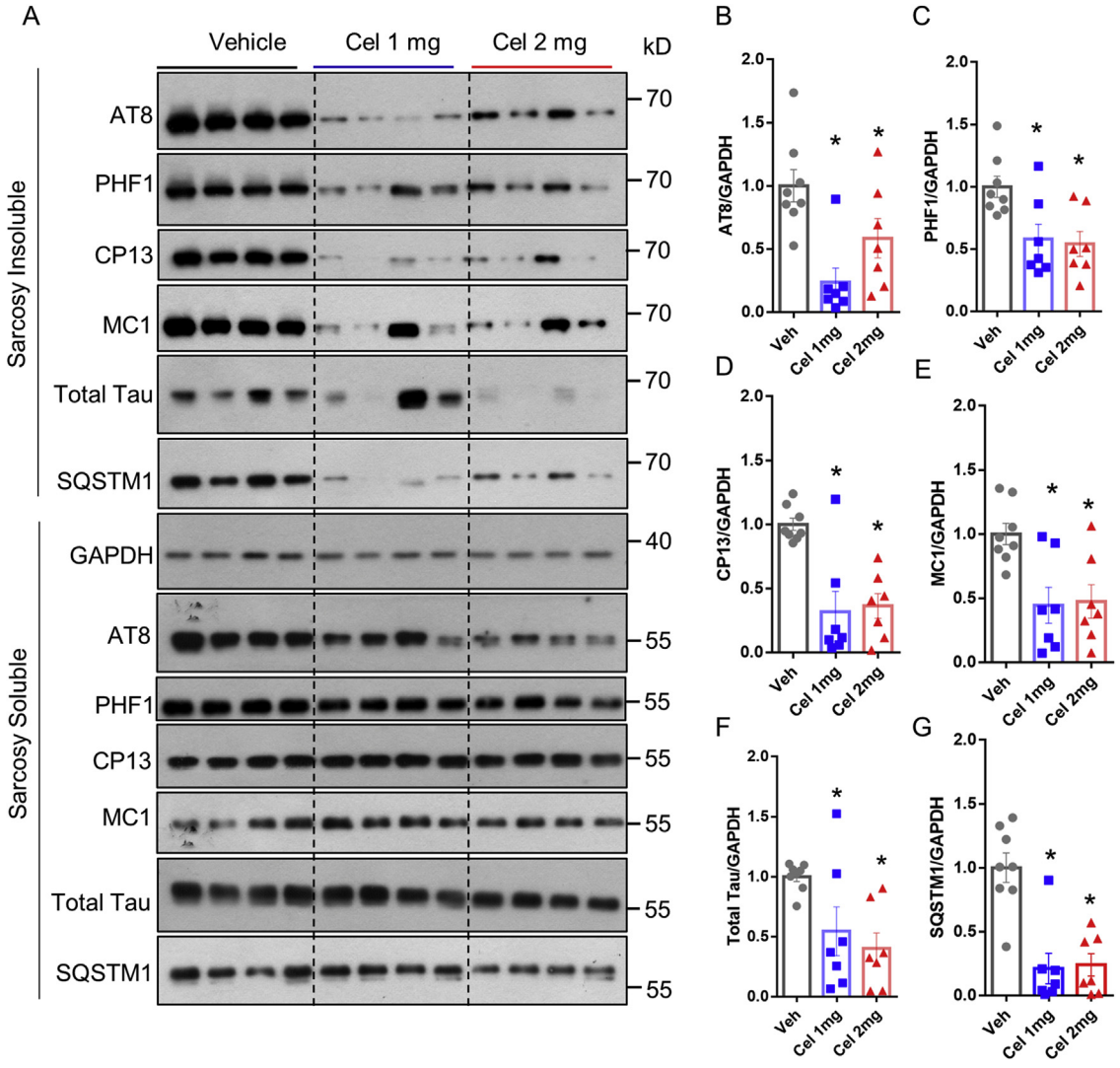

Figure 5 Celastrol reduces phosphorylated Tau aggregates in P301S Tau mice. (A) The brain lysates of P301S Tau mice in Fig. 4 were separated into sarcosyl-insoluble and sarcosyl-soluble fractions. (B−E) Phosphorylated Tau proteins (AT8, PHF1, CP13, and MC1) from sarcosyl-insoluble fractions were quantified. (F, G) Total Tau proteins and autophagy substrate SQSTM1/p62 from sarcosyl-insoluble fractions were quantified. All the values are average ± SEM ($n = 7-8$). *$P < 0.05$ *vs.* Vehicle group analyzed by one-way ANOVA.

(Fig. 2D). This evidence supports the notion that calcium and PPP3/calcineurin are not essential for celastrol to induce the nuclear accumulation of TFEB. We also tested whether okadaic acid (OA) induced inhibition of protein phosphatase 2A (PP2A) could attenuate the nuclear accumulation of TFEB after celastrol treatment because recent findings showed that PP2A is also important for TFEB dephosphorylation and nuclear accumulation[55]. As shown in Fig. 2D, inhibition of PP2A by OA did not obviously affect the nuclear accumulation of TFEB in response to celastrol, suggesting that PP2A is also not required for Celastrol-induced nuclear accumulation of TFEB. Finally, since mTORC1 is the main kinase responsible for TFEB dephosphorylation (both Ser211 and Ser142 residues)[27,36,37], we tested the effect of celastrol on mTORC1 activity. The reducing phosphorylation of RPS6KB1, a well-known downstream kinase of mTORC1, demonstrated that celastrol inhibited mTORC1 (Fig. 2E). Moreover, knockdown of the expression of TSC2 compromised the inhibition of mTORC1 in response to celastrol (Fig. 2F). These results indicate that celastrol may activate TFEB *via* inhibition of mTORC1. Together, these results demonstrate that celastrol-induced TFEB nuclear accumulation occurs *via* mTORC1 inhibition and does not involve calcium-dependent calcineurin or PP2A activation.

3.3. Celastrol activates TFEB to enhance autophagy in mouse brains

To determine whether celastrol can penetrate the BBB and enter the brain, an essential requirement for an anti-AD drug candidate, we first measured the levels of celastrol in mice brain tissues. After oral administration of celastrol (2 mg/kg body weight), pharmacokinetic parameters of celastrol in mouse brains were detected at various time points. The maximum concentration (C_{max}) 696 ng/g recorded (Fig. 3A), indicated that celastrol can effectively pass the BBB. The pharmacokinetic parameters of celastrol in the plasma were also detected (Supporting Information Fig. S2 and Table S2). Next, we wondered whether celastrol could promote TFEB-mediated autophagy and lysosomal biogenesis in

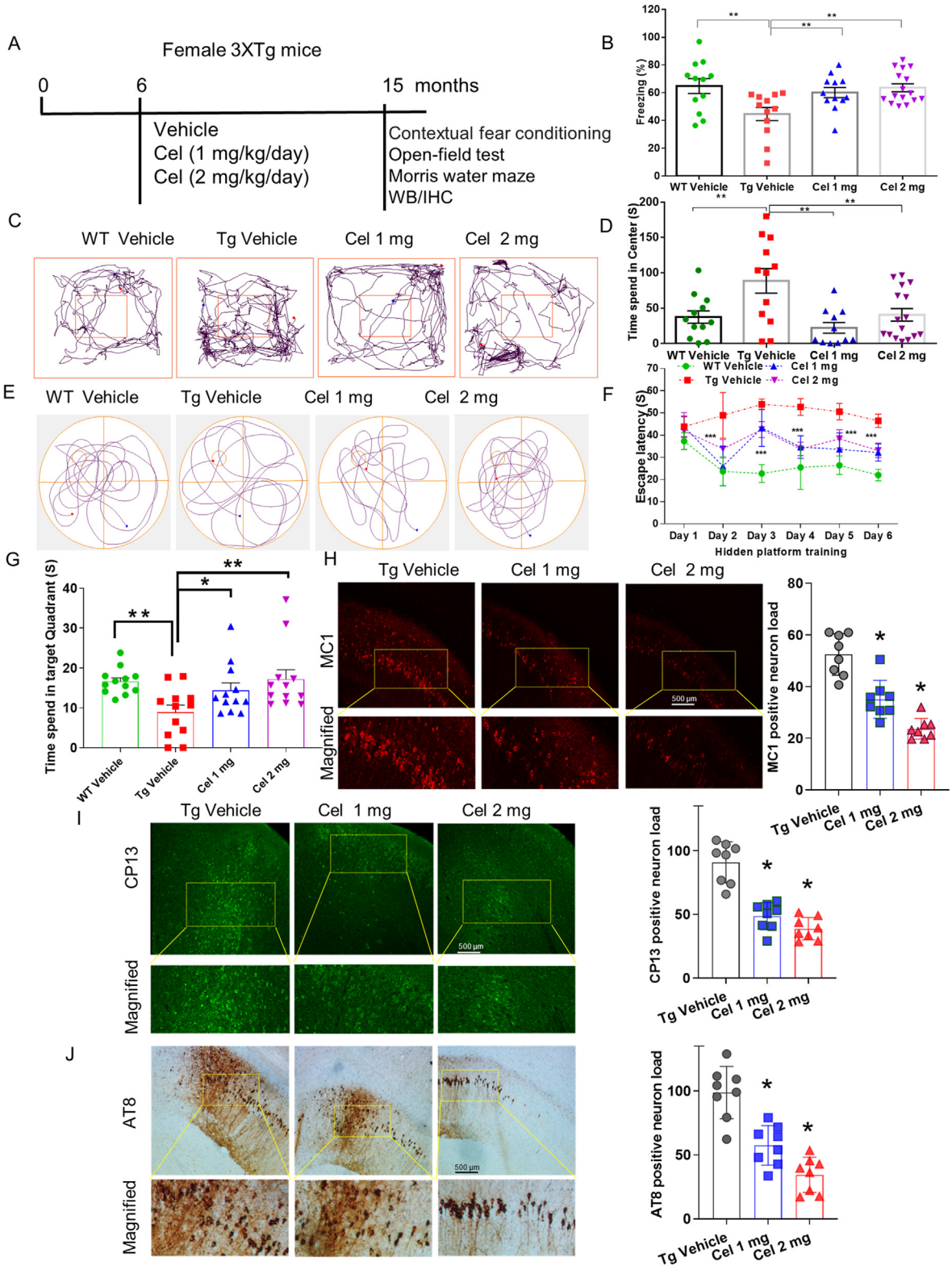

Figure 6 Celastrol mitigates memory impairments and reduces Tau aggregates in 3xTg mice. (A) Schematic models show experimental design for 3xTg mice. At the end of drug treatment, (B) contextual fear conditioning test results show that celastrol improved memory impairments. (C, D) Open field test results show that celastrol improved exploratory and locomotor behavior. (E−G) Morris water maze results show that celastrol ameliorated spatial learning and memory impairment in 3xTg mice. (H) Immunofluorescence analysis and quantification data show that celastrol reduced MC1 levels. (I) Immunofluorescence analysis and quantification data show that celastrol reduced CP13 levels. (J) Immunohistochemistry analysis and quantification data show that celastrol reduced AT8 levels (scale bar = 500 μm). All the values are average ± SEM (n = 8). *P < 0.05, **P < 0.01 *vs.* Vehicle group analyzed by one-way ANOVA.

mouse brains. After isolation of the cytoplasm and the nuclear fractions from the brains of mice that had been treated with celastrol for 7 consecutive days by gavage, Western blotting was performed, and results show that celastrol promotes TFEB translocation from the cytosol into the nucleus (Fig. 3B and C). Celastrol increased the levels of LC3B-II, pro-cathepsin B, mature-cathepsin B, pro-cathepsin D, mature-cathepsin D, and LAMP1 levels in the frontal cortex (Fig. 3D−H), suggesting that celastrol promotes TFEB-mediated autophagy and lysosomal biogenesis in mouse brains. Taken together, these results show that celastrol is BBB-permeable and promotes autophagy and lysosomal biogenesis in mouse brains.

3.4. *Celastrol attenuates Tau pathology in P301S Tau mice*

Since pharmacological or genetic activation of TFEB promotes phosphorylated Tau degradation and improves neurodegeneration in multiple AD animal models, we tested whether celastrol, a TFEB agonist, could alleviate Tau pathology in AD mice. We firstly employed homozygous P301S Tau mice, expressing four-repeat human Tau protein with the P301S mutation in nerve cells, created by Dr. Michael Goedert[38], to test the anti-AD effect of celastrol. Tau protein hyperphosphorylation and aggregation, characteristic in AD and other tauopathies are observed in these mice, and thus they are commonly used for AD study[38]. Celastrol (1 and 2 mg/kg/day) was orally administered to 1.5-month-old P301S Tau mice for 2.5 months, and then the behaviors were assessed (Fig. 4A). The percentage of freezing was significantly increased in celastrol-treated mice compared to vehicle-treated P301S Tau mice in contextual fear conditioning (CFC) test (Fig. 4B), indicating that celastrol improves learning and memory ability in these mice. An open-field test was also employed to test the effects of celastrol on improving exploratory behavior and locomotor activity in these mice. The results showed that transgenic (Tg) mice stayed much longer in the center compared with the wild type (WT) mice, and celastrol-treated mice showed reduced time in the center compared with P301S Tau mice (Fig. 4C and D). These results indicate that celastrol alleviates exploratory behavior and locomotor activity deficit in P301S Tau mice.

Next, we wondered whether celastrol-improved cognitive impairment was accompanied by reduced phosphorylated Tau levels in these mice. Immunostaining results showed that celastrol effectively reduced phosphorylated MC1 (Ser312−322) and CP13 (Ser202) levels (Fig. 4E and F). Immunohistochemistry staining using another phosphorylated Tau antibody AT8 (S202/T205) further confirmed that celastrol reduced phosphorylated Tau in P301S Tau mice (Fig. 4G). Since insoluble phosphorylated Tau contributes to neurodegeneration, we further determined whether celastrol could reduce insoluble Tau levels. Brains samples were fractionated into the detergent (sarcosyl)-soluble and -insoluble fractions according to a previous method[40,41]. Western blotting results show that celastrol specifically reduced phosphorylated Tau AT8, PHF1 (Ser396 and Ser404), CP13, conformation-specific

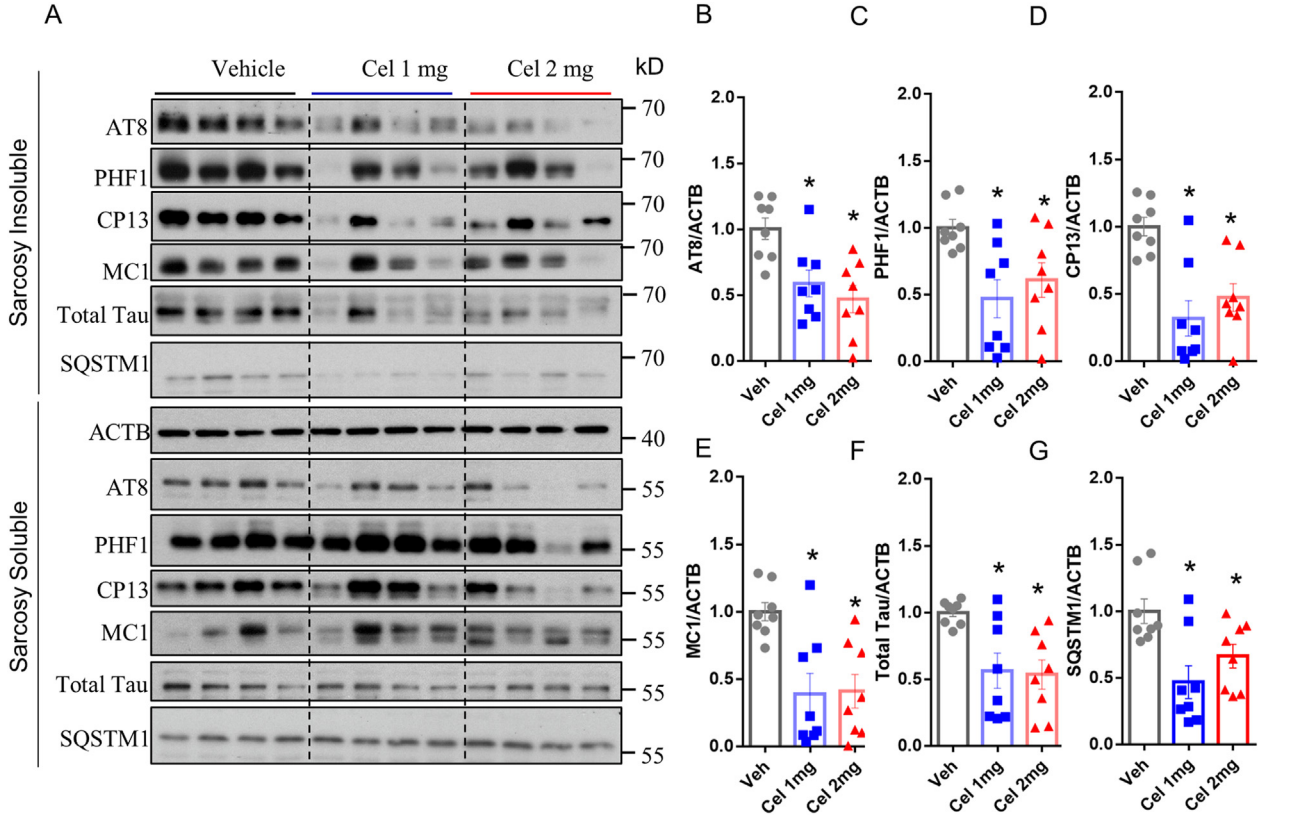

Figure 7 Celastrol reduces phosphorylated Tau aggregates in 3xTg mice. (A) The brain lysates of 3xTg mice in Fig. 6 were separated into sarcosyl-insoluble and sarcosyl-soluble fractions. (B−E) Phosphorylated Tau proteins (AT8, PHF1, CP13, and MC1) from sarcosyl-insoluble fractions were quantified. (F, G) Total Tau proteins and autophagy substrate SQSTM1/p62 from sarcosyl-insoluble fractions were quantified. All the values are average ± SEM ($n = 7$−8). *$P < 0.05$ *vs.* Vehicle group analyzed by one-way ANOVA.

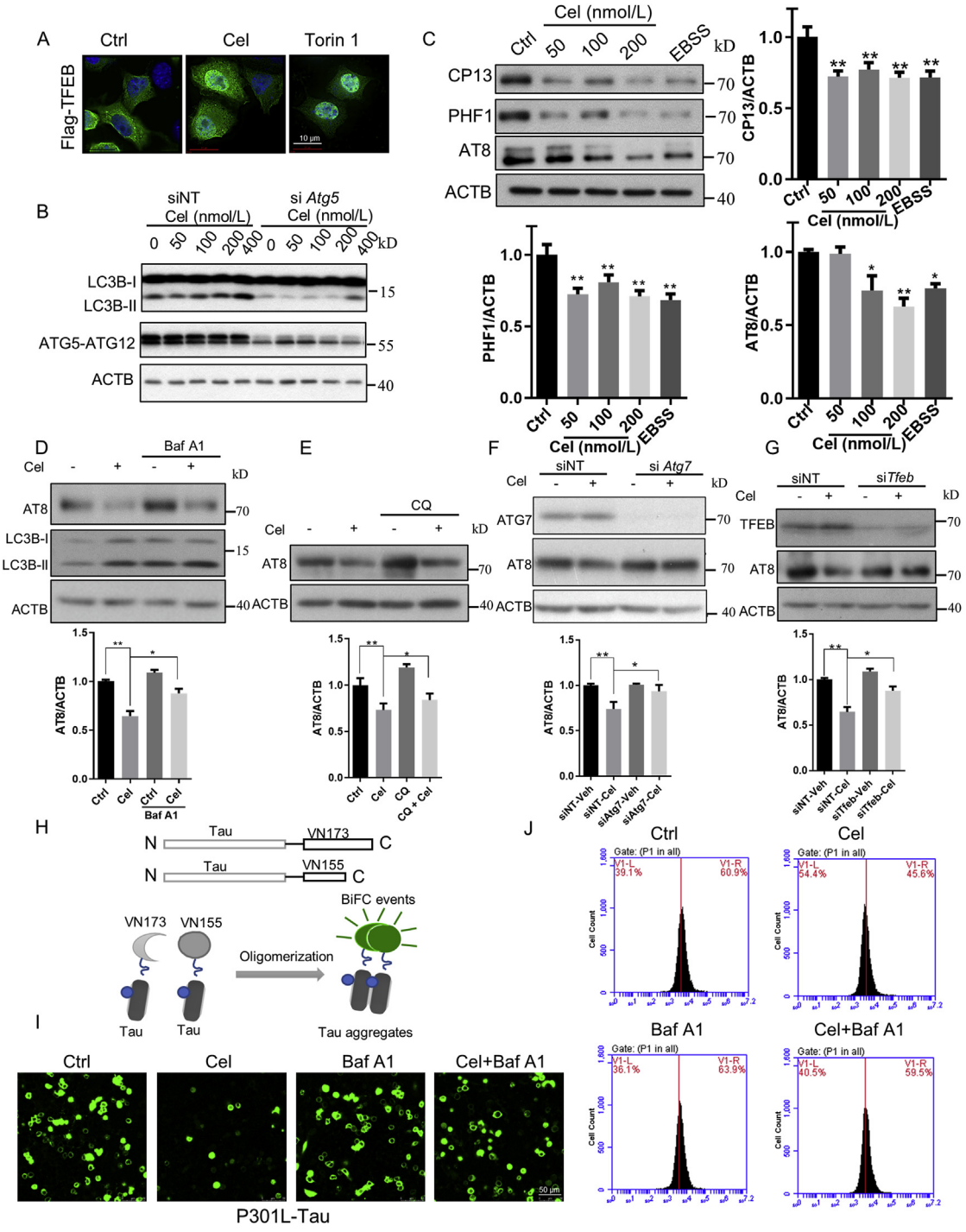

Figure 8 TFEB-mediated autophagy and the lysosomal pathway are required for celastrol-induced phosphorylated Tau aggregate degradation. (A) Celastrol promotes TFEB nucleus accumulation in mouse neuroblastoma N2a cells transiently expressing Flag-TFEB (scale bar = 10 μm). (B) Celastrol-induced autophagy in N2a cells; knockdown of *Atg5* attenuated celastrol-induced elevation of LC3B-II levels. (C) Celastrol promoted the clearance of phosphorylated Tau (CP13, PHF1, AT8) in NP40-insoluble fraction in N2a cells transiently expressing P301L Tau; starvation (EBSS) was used a positive control. (D) Celastrol increased autophagy flux; lysosome inhibitor Baf A1 attenuated SDS-insoluble phosphorylated Tau degradation in response to celastrol in N2a cells. (E) Lysosome inhibitor CQ attenuated AT8 degradation in response to celastrol in N2a cells. (F) Knockdown of *Atg7* compromised phosphorylated Tau AT8 degradation after celastrol treatment. (G) Knockdown of *Tfeb* compromised AT8 degradation after celastrol treatment. (H) Schematic models show tau-BiFC sensor based on Venus-based BiFC system. N- and C-terminal constituents of Venus protein were fused to full-length P301L mutated Tau. After Tau formed aggregates, the fluorescence increased. (I, J) By using a Tau-BiFC sensor, representative results from fluorescence microscope and flow cytometry analysis show that celastrol reduced Tau aggregates, and this reduction is inhibited by lysosome inhibitor Baf A1 (scale bar = 50 μm). All the values are average ± SEM from at least three independent experiments. $^{*}P < 0.05$, $^{**}P < 0.01$ *vs.* the control group or as indicated analyzed by one-way ANOVA.

Tau (MC1), total Tau and autophagy substrate sequestosome 1 (SQSTM1/p62) in the sarcosyl-insoluble fractions in a dose-dependent manner (Fig. 5). In contrast, celastrol had minimal effects on reducing soluble phosphorylated Tau levels (Fig. 5, quantification data not shown). These results demonstrate that celastrol may specifically reduce insoluble Tau aggregates in the brain of P301S mice. Taken together, our findings indicate that celastrol specifically reduces insoluble, phosphorylated Tau aggregates and improves memory deficiency in P301S Tau mice.

3.5. *Celastrol mitigates cognitive deficits and reduces phosphorylated Tau aggregates in 3xTg AD mice*

We next employed another Tau-associated AD animal model, the 3xTg mice, to further verify the roles of celastrol in attenuating Tau pathology. 3xTg mice harbor three human mutant genes: APP with the Swedish mutation, presenilin-1-KI, and TauP301L[56]. These mice show various characteristics of AD pathology including Tau-associated neurofibrillary tangles and Aβ-associated amyloid plaques[56]. We orally administered celastrol at the concentrations of 1 and 2 mg/kg/day to 3xTg mice from 6-month- to 15-month-old (Fig. 6A). At the end of drug administration, the CFC test, open field test, and Morris water maze (MWM) test were used to assess cognitive deficits. In the CFC test, as expected, the percentage of freezing was significantly decreased in 3xTg mice compared with wild mice (Fig. 6B). In contrast, celastrol-treated mice froze more than vehicle Tg mice (Fig. 6B), suggesting that celastrol improved learning and memory ability in these mice. In the open-field test, 3xTg mice spent more time in the center compared with WT mice, and celastrol-treated mice dramatically reversed this phenomenon compared with Tg vehicle (Fig. 6C and D), indicating that celastrol improved exploratory behavior and locomotor activity. Finally, to further verify the effects of celastrol on learning and memory, the MWM behavior test was performed. The escape latencies were determined during 6 days of hidden platform training. The results show that the escape latencies of celastrol-treated mice were significantly shorter than Tg vehicle mice (Fig. 6E−G), suggesting that celastrol improves spatial reference memory in 3xTg mice. In the probe trial, celastrol-treated mice spent a much longer time in the quadrant compared with Tg vehicle mice (Fig. 6F and G), indicating that celastrol may improve memory. Overall, these results indicate that celastrol ameliorates cognitive deficits in 3xTg mice.

We next studied whether the ability of celastrol to improve memory is related to its attenuating Tau pathology. Immunostaining and immunohistochemistry were firstly used to detect the phosphorylated Tau levels in mouse brains. The immunostaining assay (Fig. 6H and I) shows that phosphorylated Tau proteins CP13 (Ser202) and MC1 (Ser312−322) were significantly reduced after celastrol treatment. AT8 (S202/T205) levels were also dramatically reduced in response to celastrol treatment (Fig. 6J). These results suggest that celastrol reduced phosphorylated Tau levels in 3xTg mice. Since insoluble phosphorylated Tau contributes to neurodegeneration, we further determined whether celastrol could specifically reduce insoluble phosphorylated Tau in 3xTg mice. Brain samples were fractionated into the detergent (sarcosyl)-soluble and -insoluble fractions. Western blotting results showed that celastrol specifically reduced phosphorylated Tau AT8, PHF1, CP13, conformation-specific Tau MC1, total Tau, and autophagy substrate SQSQTM1/p62 in the sarcosyl-insoluble fractions in a dose-dependent manner (Fig. 7A−G). In contrast, celastrol did not noticeably affect soluble phosphorylated Tau levels (Fig. 7A). These results demonstrate that celastrol specifically reduces insoluble Tau aggregates in the brain of 3xTg mice. Taking our results together, we conclude that celastrol improves memory deficiency and reduces insoluble, phosphorylated Tau in 3xTg mice.

3.6. *TFEB-mediated autophagy is required for celastrol to degrade phosphorylated Tau in vitro*

The results in P301S Tau mice and 3xTg mice show that celastrol improves memory deficiency and reduces phosphorylated Tau aggregates in mouse brains. We next studied whether TFEB-mediated autophagy is responsible for its anti-AD effects with a particular focus on phosphorylated Tau aggregate degradation. In P301S Tau mice, results of fractionation of the cytoplasm and the nucleus fractions followed by Western blot assay showed that celastrol treatment significantly increased the accumulation of TFEB in the nucleus (Supporting Information Fig. S3A and S3B). Interestingly, celastrol also increased mature cathepsin B (m-CTSB), and mature cathepsin D (m-CTSD) levels in the brain of P301S Tau mice (Fig. S3C and S3D), suggesting that celastrol activates TFEB to induce autophagy in pathological conditions of animal brains. Moreover, in both 3xTg and P301S Tau mice, celastrol increased autophagy marker LC3B-II (Fig. S3E and S3F) and reduced SQSTM1/p62 levels (Figs. 5 and 7), suggesting that celastrol promotes autophagy in Tg mice and that the enhancement of autophagy may contribute to its effects in reducing phosphorylated Tau levels.

To confirm whether TFEB-mediated autophagy is responsible for phosphorylated Tau degradation, we first examined whether celastrol can activate TFEB in neuron cell line N2a cells. As shown in Fig. 8A, celastrol promoted the nuclear accumulation of TFEB and increased the expression of LC3B-II (Fig. 8B). Knockdown of *ATG5* attenuated celastrol-induced the increase of LC3B-II levels (Fig. 8B). Importantly, celastrol further increased LC3B-II levels in the presence of lysosomal inhibitor Baf A1 (Fig. 8D), suggesting that celastrol enhances autophagy flux in neuronal N2a cells. Next, we examined whether celastrol promotes the degradation of phosphorylated Tau in N2a cells and investigated the possible mechanisms. As shown in Fig. 8C, celastrol reduced the phosphorylated Tau AT8, PHF1, and CP13 in NP40-insoluble fractions. Importantly, celastrol-mediated reduction of Tau can be inhibited by lysosomal inhibitors Baf A1 and CQ (Fig. 8D and E), suggesting that lysosome functions may be required for phosphorylated Tau aggregate degradation in response to celastrol. Furthermore, knockdown of *Atg7* and *Tfeb* also compromised celastrol-induced phosphorylated Tau degradation (Fig. 8F and G), suggesting that TFEB-mediated autophagy is required for celastrol-mediated phosphorylated Tau aggregate degradation. Finally, we used a previously described Venus-based Tau-BiFC system[49] to further verify whether celastrol could promote the degradation of Tau aggregates. In this system, wild-type full-length human Tau or P301S mutation human Tau were fused to a non-fluorescent N-terminal fragment of Venus (VN173, 1−172 a.a.) and non-fluorescent C-terminal fragment of Venus (VC155, 155−238 a.a.). After transfection into cells, the fluorescence intensity could be used as an indicator for Tau aggregate formation[49] (Fig. 8H). We used the P310L Tau-BiFC system to further examine whether celastrol promotes Tau aggregate degradation. Interestingly, we found that celastrol treatment reduced fluorescence and, importantly, lysosome inhibitor Baf A1 reversed this effect in the P301L Tau-BiFC system as shown in

microscope images (Fig. 8I). Flow cytometry-based assay further confirmed the role of celastrol in promoting Tau-aggregates degradation and its susceptibility to lysosome inhibitor Baf A1 (Fig. 8J). Collectively, these results demonstrate that TFEB-mediated autophagy is required for phosphorylated Tau-aggregates degradation, at least in cell models.

4. Discussion

Here, for the first time, we show that celastrol promotes TFEB-mediated autophagy and lysosomal biogenesis both *in vitro* and *in vivo*. Celastrol ameliorated memory deficiency and reduced phosphorylated Tau aggregates in P301S Tau and 3xTg mice. We also demonstrated that TFEB-mediated autophagy is required for celastrol to degrade phosphorylated Tau aggregates. These results indicate that celastrol is a novel TFEB activator that promotes the degradation of phosphorylated Tau aggregates to alleviate Tau pathology. Our findings may provide novel insight into the role of celastrol in ameliorating AD disease.

Natural products represent an important resource for developing effective agents for treating aging-associated diseases including neurodegenerative diseases[57,58]. We previously identified several natural autophagy activators and showed neuroprotective effects in neurodegenerative disease cell/animal models[37,40,59,60]. Celastrol, a natural triterpenoid, has multiple biological activities including anti-inflammatory, anti-cancer, anti-obesity, and anti-diabetic effects[32−35,61]. Here, we uncovered an additional potential activity: that of preventing or reducing neurodegeneration. Tau pathology is a key characteristic of AD; our findings suggest that celastrol can reduce Tau pathology. Tau is a microtubule-associated protein abundantly expressed in the axons of neurons. A main function of Tau is stabilizing microtubules[62]. In AD and other Tau-related neurodegenerative diseases, Tau proteins are hyperphosphorylated and form insoluble aggregates, thus losing the ability to stabilize microtubule, leading to axonal transport impairment, and finally neuron death and, by association, cognitive deficits[62]. Interestingly, mounting evidence suggests that Tau pathology better correlates with cognitive impairment than Aβ in AD. As such, targeting pathological Tau is a promising strategy for developing pharmaceutical interventions of AD and other tauopathies. Among all the strategies, enhancing autophagy by targeting TFEB to degrade phosphorylated Tau aggregates is an effective way to prevent pathological disease. Our findings in animal models show that TFEB activator celastrol may represent a novel agent for preventing/treating AD by degradation of phosphorylated Tau aggregates.

Previous studies have shown that celastrol-induced heat shock response and the upregulation of chaperones are responsible for its neuroprotective effects in neurodegenerative diseases such as Huntington's disease and amyotrophic lateral sclerosis[63−65]. Previous studies on these diseases suggest that celastrol has neuroprotective effects in AD *via* a mechanism related to reducing beta-amyloid pathology *via* inhibiting BACE-1 activity[66]. However, the role and underlying mechanisms of celastrol in attenuating Tau-pathology have not been reported. Here, we have revealed that celastrol promotes the degradation of phosphorylated Tau aggregates *via* a novel mechanism involving TFEB-mediated autophagy and improves AD-associated memory deficiency in mouse models. Future studies using brain-specific TFEB knockout and/or autophagy-deficient mice to further explore the underlying mechanism of celastrol in alleviating Tau pathology in the animal models are required to confirm the neuroprotective effects of celastrol. Since previous reports showed that chaperones also play a role in the clearing of Tau proteins, we cannot fully exclude the possibility that celastrol-induced heat shock response and the upregulating expression of chaperones also plays a role in its ability to alleviate Tau pathology in P301S Tau and 3xTg mice. Though we have revealed that celastrol promotes Tau degradation, alleviates memory deficiency, and induces autophagy in 3XTg mice, the role of celastrol in reducing beta-amyloid pathology may also be responsible for its effect in improving memory deficit since it has been reported that celastrol reduced Aβ production[66]. Our results in 5xFAD mice also showed that celastrol alleviates Aβ pathology (data not shown). Here, we have found that celastrol induces autophagy *via* mTORC1 inhibition-mediated TFEB dephosphorylation and activation. These results suggest that celastrol may have multiple targets for inducing autophagy. Nevertheless, the drug target for celastrol-mediated mTORC1 inhibition is still elusive; future studies are required for determining this target. Since celastrol has anti-inflammatory effects[33], an inflammatory response is also critical for AD pathogenesis, it is also possible that these effects also play a role in alleviating AD pathology in response to celastrol treatment. Finally, mitophagy has been implicated in the pathogenesis of multiple diseases including AD[67−69], whether mitophagy may also play a role in alleviating AD are unclear since celastrol was reported to activate TFEB[33]. Future studies aiming at understanding this question is an interesting topic.

5. Conclusions

Overall, given that the impairment of the autophagy−lysosomal pathway has been connected to the pathogenesis of numerous diseases such as liver diseases, AD[31,56,70−72], and other tauopathies, and that autophagy plays a critical role in the degradation of phosphorylated Tau aggregates to alleviate disease pathology. Thus, autophagy enhancers, especially those targeting TFEB, hold great promise for developing novel anti-AD agents. Here, we found celastrol promoted the degradation of phosphorylated Tau aggregates in P301S Tau and 3xTg mice and improved memory deficits apparently *via* activating TFEB-mediated autophagy. Thus, the results here provide strong justification for the future development of celastrol as a novel pharmaceutical agent. Our study may enhance understanding of the pharmacological activation of TFEB to degrade phosphorylated Tau aggregates and point to a new strategy for the discovery and development of drugs to treat and/or prevent AD and other tauopathies.

Acknowledgments

We would like to thank Prof. Myung-Shik Lee (Yonsei University College of Medicine, Seoul, South Korea) and Prof. Richard J. Youle (US National Institute of Neurological Disorders and Stroke, Bethesda, MD, USA) for providing *TFEB* knockout HeLa cells. We thank Martha Dahlen for the English editing. This study was supported by the research fund from Hong Kong Baptist University (HKBU/RC-IRCs/17-18/03, China), Hong Kong General Research Fund (GRF/HKBU12101417 and GRF/HKBU12100618, China), the National Natural Science Foundation of China (81703487 and 81773926), Shenzhen Science and Technology Innovation Commission (JCYJ20180302174028790, JCYJ20180507184656626,

and JCYJ20210324114014039, China), and the Hong Kong Health and Medical Research Fund (HMRF17182541 and HMRF17182551, China).

Author contributions

Chuanbin Yang, Min Li, and Juxian Song designed the research and supervised the project. Chuanbin Yang, Chengfu Su, Ashok Iyaswamy, Senthil Kumar Krishnamoorthi, Zhou Zhu, and Sichang Yang performed the research and analyzed the data. Chuanbin Yang and Chengfu Su drafted the manuscript and organized the figures. Benjamin Chunkit Tong, Jia Liu, Sravan G. Sreenivasmurthy, Xinjie Guan, Yuxuan Kan, Aston Jiaxi Wu, and Alexis Shiying Huang helped organize the experiment and provided technical support. Chuanbin Yang, Min Li, Juxian Song, Chengfu Su, Jieqiong Tan, and Kingho Cheung revised the manuscript. All authors have given approval to the final version of the manuscript.

Conflicts of interest

The authors have declared that there are no conflicts of interest.

Appendix A. Supporting information

Supporting data to this article can be found online at https://doi.org/10.1016/j.apsb.2022.01.017.

References

1. 2020 Alzheimer's disease facts and figures. *Alzheimers Dement* 2020;**16**:391−460.
2. Hardy J. A hundred years of Alzheimer's disease research. *Neuron* 2006;**52**:3−13.
3. Liu J, Zhang Y, Liu A, Wang J, Li L, Chen X, et al. Distinct dasatinib-induced mechanisms of apoptotic response and exosome release in imatinib-resistant human chronic myeloid leukemia cells. *Int J Mol Sci* 2016;**17**:531.
4. Iyaswamy A, Krishnamoorthi SK, Zhang H, Sreenivasmurthy SG, Zhu Z, Liu J, et al. Qingyangshen mitigates amyloid-β and Tau aggregate defects involving PPARα-TFEB activation in transgenic mice of Alzheimer's disease. *Phytomedicine* 2021;**91**:153648.
5. Walsh S, Merrick R, Milne R, Brayne C. Aducanumab for Alzheimer's disease?. *BMJ* 2021;**374**:n1682.
6. Giacobini E, Gold G. Alzheimer disease therapy—moving from amyloid-β to tau. *Nat Rev Neurol* 2013;**9**:677−86.
7. Bloom GS. Amyloid-β and tau: the trigger and bullet in Alzheimer disease pathogenesis. *JAMA Neurol* 2014;**71**:505−8.
8. Nixon RA. The role of autophagy in neurodegenerative disease. *Nat Med* 2013;**19**:983.
9. Menzies FM, Fleming A, Rubinsztein DC. Compromised autophagy and neurodegenerative diseases. *Nat Rev Neurosci* 2015;**16**:345.
10. Menzies FM, Fleming A, Caricasole A, Bento CF, Andrews SP, Ashkenazi A, et al. Autophagy and neurodegeneration: pathogenic mechanisms and therapeutic opportunities. *Neuron* 2017;**93**:1015−34.
11. Kumar H, Kim IS, More SV, Kim BW, Choi DK. Natural product-derived pharmacological modulators of Nrf2/ARE pathway for chronic diseases. *Nat Prod Rep* 2014;**31**:109−39.
12. Mbaveng AT, Kuete V, Efferth T. Potential of central, eastern and western Africa medicinal plants for cancer therapy: spotlight on resistant cells and molecular targets. *Front Pharmacol* 2017;**8**:343.
13. Pickford F, Masliah E, Britschgi M, Lucin K, Narasimhan R, Jaeger PA, et al. The autophagy-related protein beclin 1 shows reduced expression in early Alzheimer disease and regulates amyloid β accumulation in mice. *J Clin Invest* 2008;**118**:2190−9.
14. Ni HM, Chao X, Yang H, Deng F, Wang S, Bai Q, et al. Dual roles of mammalian target of rapamycin in regulating liver injury and tumorigenesis in autophagy-defective mouse liver. *Hepatology* 2019;**70**:2142−55.
15. Ni HM, McGill MR, Chao X, Du K, Williams JA, Xie Y, et al. Removal of acetaminophen protein adducts by autophagy protects against acetaminophen-induced liver injury in mice. *J Hepatol* 2016;**65**:354−62.
16. Di Meco A, Curtis ME, Lauretti E, Praticò D. Autophagy dysfunction in Alzheimer's disease: mechanistic insights and new therapeutic opportunities. *Biol Psychiatr* 2020;**87**:797−807.
17. Li Q, Liu Y, Sun M. Autophagy and Alzheimer's disease. *Cell Mol Neurobiol* 2017;**37**:377−88.
18. Leidal AM, Levine B, Debnath J. Autophagy and the cell biology of age-related disease. *Nat Cell Biol* 2018;**20**:1338−48.
19. Yang C, Cai CZ, Song JX, Tan JQ, Durairajan SSK, Iyaswamy A, et al. NRBF2 is involved in the autophagic degradation process of APP-CTFs in Alzheimer disease models. *Autophagy* 2017;**13**:2028−40.
20. Lachance V, Wang Q, Sweet E, Choi I, Cai CZ, Zhuang XX, et al. Autophagy protein NRBF2 has reduced expression in Alzheimer's brains and modulates memory and amyloid-beta homeostasis in mice. *Mol Neurodegener* 2019;**14**:43.
21. Ouyang X, Ahmad I, Johnson MS, Redmann M, Craver J, Wani WY, et al. Nuclear receptor binding factor 2 (NRBF2) is required for learning and memory. *Lab Invest* 2020;**100**:1238−51.
22. Cai CZ, Yang C, Zhuang XX, Yuan NN, Wu MY, Tan JQ, et al. NRBF2 is a RAB7 effector required for autophagosome maturation and mediates the association of APP-CTFs with active form of RAB7 for degradation. *Autophagy* 2021;**17**:1112−30.
23. Jaeger PA, Wyss-Coray T. Beclin 1 complex in autophagy and Alzheimer disease. *Arch Neurol* 2010;**67**:1181−4.
24. Nilsson P, Loganathan K, Sekiguchi M, Matsuba Y, Hui K, Tsubuki S, et al. Aβ secretion and plaque formation depend on autophagy. *Cell Rep* 2013;**5**:61−9.
25. Nilsson P, Sekiguchi M, Akagi T, Izumi S, Komori T, Hui K, et al. Autophagy-related protein 7 deficiency in amyloid β (Aβ) precursor protein transgenic mice decreases Aβ in the multivesicular bodies and induces Aβ accumulation in the Golgi. *Am J Pathol* 2015;**185**:305−13.
26. Hung SY, Huang WP, Liou HC, Fu WM. LC3 overexpression reduces Aβ neurotoxicity through increasing α7nAchR expression and autophagic activity in neurons and mice. *Neuropharmacology* 2015;**93**:243−51.
27. Settembre C, Di Malta C, Polito VA, Arencibia MG, Vetrini F, Erdin S, et al. TFEB links autophagy to lysosomal biogenesis. *Science* 2011;**332**:1429−33.
28. Sardiello M, Palmieri M, di Ronza A, Medina DL, Valenza M, Gennarino VA, et al. A gene network regulating lysosomal biogenesis and function. *Science* 2009;**325**:473−7.
29. Martina JA, Chen Y, Gucek M, Puertollano R. MTORC1 functions as a transcriptional regulator of autophagy by preventing nuclear transport of TFEB. *Autophagy* 2012;**8**:903−14.
30. Polito VA, Li H, Martini-Stoica H, Wang B, Yang L, Xu Y, et al. Selective clearance of aberrant tau proteins and rescue of neurotoxicity by transcription factor EB. *EMBO Mol Med* 2014;**6**:1142−60.
31. Martini-Stoica H, Xu Y, Ballabio A, Zheng H. The autophagy−lysosomal pathway in neurodegeneration: a TFEB perspective. *Trends Neurosci* 2016;**39**:221−34.
32. Cascão R, Fonseca JE, Moita LF. Celastrol: a spectrum of treatment opportunities in chronic diseases. *Front Med (Lausanne)* 2017;**4**:69.
33. Hu M, Luo Q, Alitongbieke G, Chong S, Xu C, Xie L, et al. Celastrol-induced Nur77 interaction with TRAF2 alleviates inflammation by promoting mitochondrial ubiquitination and autophagy. *Mol Cell* 2017;**66**:141−153.e6.

34. Liu J, Lee J, Hernandez MAS, Mazitschek R, Ozcan U. Treatment of obesity with celastrol. *Cell* 2015;**161**:999−1011.
35. Ma X, Xu L, Alberobello AT, Gavrilova O, Bagattin A, Skarulis M, et al. Celastrol protects against obesity and metabolic dysfunction through activation of a HSF1−PGC1α transcriptional axis. *Cell Metab* 2015;**22**:695−708.
36. Settembre C, Zoncu R, Medina DL, Vetrini F, Erdin S, Erdin S, et al. A lysosome-to-nucleus signalling mechanism senses and regulates the lysosome *via* mTOR and TFEB. *EMBO J* 2012;**31**:1095−108.
37. Song JX, Sun YR, Peluso I, Zeng Y, Yu X, Lu JH, et al. A novel curcumin analog binds to and activates TFEB *in vitro* and *in vivo* independent of MTOR inhibition. *Autophagy* 2016;**12**:1372−89.
38. Allen B, Ingram E, Takao M, Smith MJ, Jakes R, Virdee K, et al. Abundant tau filaments and nonapoptotic neurodegeneration in transgenic mice expressing human P301S tau protein. *J Neurosci* 2002;**22**:9340−51.
39. Dennison JL, Ricciardi NR, Lohse I, Volmar CH, Wahlestedt C. Sexual dimorphism in the 3xTg-AD mouse model and its impact on pre-clinical research. *J Alzheimers Dis* 2021;**80**:41−52.
40. Song JX, Malampati S, Zeng Y, Durairajan SSK, Yang CB, Tong BC, et al. A small molecule transcription factor EB activator ameliorates beta-amyloid precursor protein and Tau pathology in Alzheimer's disease models. *Aging Cell* 2020;**19**:e13069.
41. Iyaswamy A, Krishnamoorthi SK, Song JX, Yang CB, Kaliyamoorthy V, Zhang H, et al. NeuroDefend, a novel Chinese medicine, attenuates amyloid-β and tau pathology in experimental Alzheimer's disease models. *J Food Drug Anal* 2020;**28**:132−46.
42. Kraeuter AK, Guest PC, Sarnyai Z. The open field test for measuring locomotor activity and anxiety-like behavior. *Methods Mol Biol* 2019; **1916**:99−103.
43. Rudy JW, O'Reilly RC. Contextual fear conditioning, conjunctive representations, pattern completion, and the hippocampus. *Behav Neurosci* 1999;**113**:867−80.
44. Bromley-Brits K, Deng Y, Song W. Morris water maze test for learning and memory deficits in Alzheimer's disease model mice. *J Vis Exp* 2011;**53**:e2920.
45. Yang C, Zhu Z, Tong BCK, Iyaswamy A, Xie WJ, Zhu Y, et al. A stress response p38 MAP kinase inhibitor SB202190 promoted TFEB/TFE3-dependent autophagy and lysosomal biogenesis independent of p38. *Redox Biol* 2020;**32**:101445.
46. Zheng X, Lin W, Jiang Y, Lu K, Wei W, Huo Q, et al. Electroacupuncture ameliorates beta-amyloid pathology and cognitive impairment in Alzheimer disease *via* a novel mechanism involving activation of TFEB (transcription factor EB). *Autophagy* 2021;**17**: 3833−47.
47. Yang C, Zhao J, Cheng Y, Le XC, Rong J. *N*-Propargyl caffeate amide (PACA) potentiates nerve growth factor (NGF)-induced neurite outgrowth and attenuates 6-hydroxydopamine (6-OHDA)-induced toxicity by activating the Nrf2/HO-1 pathway. *ACS Chem Neurosci* 2015;**6**:1560−9.
48. Yang CB, Liu J, Tong BC, Wang ZY, Zhu Z, Su CF, et al. TFEB, a master regulator of autophagy and biogenesis, unexpectedly promotes apoptosis in response to the cyclopentenone prostaglandin 15d-PGJ2. *Acta Pharmacol Sin* 2021. Available from: https://doi.org/10.1038/s41401-021-00711-7.
49. Tak H, Haque MM, Kim MJ, Lee JH, Baik JH, Kim Y, et al. Bimolecular fluorescence complementation; lighting-up tau−tau interaction in living cells. *PLoS One* 2013;**8**:e81682.
50. Settembre C, Medina DL. TFEB and the CLEAR network. *Methods Cell Biol* 2015;**126**:45−62.
51. Klionsky DJ, Abdel-Aziz AK, Abdelfatah S, Abdellatif M, Abdoli A, Abel S, et al. Guidelines for the use and interpretation of assays for monitoring autophagy (4th edition)[1]. *Autophagy* 2021;**17**:1−382.
52. Puertollano R, Ferguson SM, Brugarolas J, Ballabio A. The complex relationship between TFEB transcription factor phosphorylation and subcellular localization. *EMBO J* 2018;**37**:e98804.
53. Medina DL, Di Paola S, Peluso I, Armani A, De Stefani D, Venditti R, et al. Lysosomal calcium signalling regulates autophagy through calcineurin and TFEB. *Nat Cell Biol* 2015;**17**:288−99.
54. Liu J, Farmer Jr JD, Lane WS, Friedman J, Weissman I, Schreiber SL. Calcineurin is a common target of cyclophilin−cyclosporin A and FKBP−FK506 complexes. *Cell* 1991;**66**:807−15.
55. Martina JA, Puertollano R. Protein phosphatase 2A stimulates activation of TFEB and TFE3 transcription factors in response to oxidative stress. *J Biol Chem* 2018;**293**:12525−34.
56. Wang S, Ni HM, Chao X, Wang H, Bridges B, Kumer S, et al. Impaired TFEB-mediated lysosomal biogenesis promotes the development of pancreatitis in mice and is associated with human pancreatitis. *Autophagy* 2019;**15**:1954−69.
57. Yang C, Zhang W, Dong X, Fu C, Yuan J, Xu M, et al. A natural product solution to aging and aging-associated diseases. *Pharmacol Ther* 2020;**216**:107673.
58. Iyaswamy A, Krishnamoorthi SK, Liu YW, Song J, Kammala AK, Sreenivasmurthy SG, et al. Yuan-Hu Zhi Tong Prescription mitigates tau pathology and alleviates memory deficiency in the preclinical models of Alzheimer's disease. *Front Pharmacol* 2020;**11**: 584770.
59. Wang Z, Yang C, Liu J, Chun-Kit Tong B, Zhu Z, Malampati S, et al. A curcumin derivative activates TFEB and protects against parkinsonian neurotoxicity *in vitro*. *Int J Mol Sci* 2020;**21**:1515.
60. Song JX, Lu JH, Liu LF, Chen LL, Durairajan SS, Yue Z, et al. HMGB1 is involved in autophagy inhibition caused by SNCA/α-synuclein overexpression: a process modulated by the natural autophagy inducer corynoxine B. *Autophagy* 2014;**10**:144−54.
61. Feng X, Guan D, Auen T, Choi JW, Salazar Hernández MA, Lee J, et al. IL1R1 is required for celastrol's leptin-sensitization and anti-obesity effects. *Nat Med* 2019;**25**:575−82.
62. Bakota L, Brandt R. Tau biology and tau-directed therapies for Alzheimer's disease. *Drugs* 2016;**76**:301−13.
63. Westerheide SD, Bosman JD, Mbadugha BN, Kawahara TL, Matsumoto G, Kim S, et al. Celastrols as inducers of the heat shock response and cytoprotection. *J Biol Chem* 2004;**279**:56053−60.
64. Zhang YQ, Sarge KD. Celastrol inhibits polyglutamine aggregation and toxicity though induction of the heat shock response. *J Mol Med (Berl)* 2007;**85**:1421−8.
65. Kiaei M, Kipiani K, Petri S, Chen J, Calingasan NY, Beal MF. Celastrol blocks neuronal cell death and extends life in transgenic mouse model of amyotrophic lateral sclerosis. *Neurodegener Dis* 2005;**2**:246−54.
66. Paris D, Ganey NJ, Laporte V, Patel NS, Beaulieu-Abdelahad D, Bachmeier C, et al. Reduction of beta-amyloid pathology by celastrol in a transgenic mouse model of Alzheimer's disease. *J Neuroinflammation* 2010;**7**:17.
67. Ni HM, Williams JA, Ding WX. Mitochondrial dynamics and mitochondrial quality control. *Redox Biol* 2015;**4**:6−13.
68. Wang L, Qi H, Tang Y, Shen HM. Post-translational modifications of key machinery in the control of mitophagy. *Trends Biochem Sci* 2020; **45**:58−75.
69. Qian H, Chao X, Williams J, Fulte S, Li T, Yang L, et al. Autophagy in liver diseases: a review. *Mol Aspects Med* 2021;**82**:100973.
70. Chao X, Wang S, Zhao K, Li Y, Williams JA, Li T, et al. Impaired TFEB-mediated lysosome biogenesis and autophagy promote chronic ethanol-induced liver injury and steatosis in mice. *Gastroenterology* 2018;**155**:865−879.e12.
71. Wang S, Ni HM, Chao X, Ma X, Kolodecik T, De Lisle R, et al. Critical role of TFEB-mediated lysosomal biogenesis in alcohol-induced pancreatitis in mice and humans. *Cell Mol Gastroenterol Hepatol* 2020;**10**:59−81.
72. Chao X, Ni HM, Ding WX. Insufficient autophagy: a novel autophagic flux scenario uncovered by impaired liver TFEB-mediated lysosomal biogenesis from chronic alcohol-drinking mice. *Autophagy* 2018;**14**: 1646−8.